Nat Hazards (2013) 65:41–62
DOI 10.1007/s11069-012-0344-9

ORIGINAL PAPER

A systematic approach for the assessment of flooding hazard and risk associated with a landslide dam

Sheng-Hsueh Yang · Yii-Wen Pan · Jia-Jyun Dong · Keh-Chia Yeh · Jyh-Jong Liao

Received: 18 March 2012 / Accepted: 2 August 2012 / Published online: 18 August 2012
© Springer Science+Business Media B.V. 2012

Abstract Inundation caused by landslide dams may occur in the upstream and downstream of the dams. A proper flooding hazard assessment is required for reaction planning and decision-making to mitigate possible flooding hazards caused by landslide dams. Both quick and detailed procedures can be used to evaluate inundation hazards, depending on the available time and information. This paper presents a systematic approach for the assessment of inundation hazards and risks caused by landslide dam formation and breaches. The approach includes the evaluation of dam-breach probability, assessment of upstream inundation hazard, assessment of downstream inundation hazard, and the classification of flooding risk. The proposed assessment of upstream inundation estimates the potential region of inundation and predicts the overtopping time. The risk level of downstream flooding is evaluated using a joint consideration of the breach probability of a landslide dam and the level of flooding hazard, which is classified using a flooding hazard index that indicates the risk of potential inundation. This paper proposes both quick and detailed procedures for the assessments of inundation in both the upstream and downstream of a landslide dam. An example of a landslide dam case study in southern Taiwan was used to demonstrate the applicability of the systematic approach.

Keywords Landslide dam · Flooding hazard · Hazard classification · Barrier Lake · Dam breach

S.-H. Yang
Disaster Prevention and Water Environment Research Center, National Chiao Tung University, 1001, University Road, Hsinchu 30010, Taiwan

Y.-W. Pan (✉) · K.-C. Yeh · J.-J. Liao
Department of Civil Engineering, National Chiao Tung University, 1001, University Road, Hsinchu 30010, Taiwan
e-mail: ywpan@mail.nctu.edu.tw

J.-J. Dong
Graduate Institute of Applied Geology, National Central University, 300, Jhongda Rd., Jhongli, Taoyuan 32001, Taiwan

1 Introduction

Landslide dams occur in numerous regions worldwide and result in considerable flooding hazards (Schuster 1995). Inundation caused by landslide dams may occur in the upstream and/or downstream of landslide dams. Upstream flooding may occur because of the gradual increase in the water level in the barrier lake before the fill-up of the lake. Conversely, the downstream inundation hazard is caused by the outburst flow after the breach of a landslide dam. Depending on the available time to respond, appropriate reaction plans and decision-making based on proper hazard assessment are essential for hazard mitigation; the prompt assessment of potential hazards is a crucial issue.

Schuster and Costa (1986) and Peng and Zhang (2012) indicated that 44–51 % of landslide dams will fail in 1 week, 59–71 % will fail in 1 month, and 83 % will fail in 6 months. The allowable response time to implement a hazard mitigation plan is often limited. A prompt (quick) assessment of inundation hazards caused by a landslide dam event is necessary in the early phase after emergent data collection and site investigation. A quick assessment must only require minimal available data and use simple and quick procedures to evaluate the threat-level of a landslide dam event. A detailed analysis can be conducted if a landslide dam survives for a sufficient period to gather sufficient data and information.

An empirical approach was proposed to classify the risk level of a landslide dam during the 2009 Wenchuan earthquake in China (Cui et al. 2009; Xu et al. 2009; Yin et al. 2009). The approach classified the risk of the landslide dam into four levels, as follows: (1) extremely high risk, (2) high risk, (3) medium risk, and (4) low risk. This classification was conducted by considering the dam height, the lake storage capacity, and the materials of the dam. However, the dam-breach probability and the consequence of outburst flooding were not separately considered in this approach. In general, it is difficult to correctly characterize the material composition of a landslide dam in a short time in the early phase. The breach probability of a landslide dam mainly depends on the geomorphic and hydrological parameters of the dam (Dong et al. 2011a, b). The in-flow peak discharge substantially affects the breach probability of a landslide dam. Conversely, the peak discharge of the flow outburst from a breached dam plays a crucial role in the level of the downstream flooding hazard.

This paper proposes a systematic approach for quick hazard evaluation followed by a detailed hazard evaluation (when possible). This approach contains four elements, that is, evaluation of dam-breach probability, assessment of upstream inundation hazard, assessment of downstream inundation hazard, and risk classification. The dam-breach probability can be evaluated using a logistic regression model that uses only the geomorphic parameters of the landslide dam; subsequently, the probability of dam breach can be classified into various levels. The upstream inundation hazard is assessed by the rising water stage in the barrier lake that is dammed by a landslide dam. The downstream inundation hazard is evaluated by considering the outburst flood from the breached dam. Quick and detail procedures can be used to assess the inundation hazard. The inundation hazard can be classified into various levels regarding the seriousness of flooding. The risk level of a landslide dam on the downstream inundation is the joint results of dam breach and downstream flooding; thus, it can be combined and classified according to the level of dam-breach probability and the level of flooding hazard. All of the elements of the systematic procedure are presented in order. Finally, a case study of a landslide dam in southern Taiwan is presented to demonstrate the feasibility of the systematic approach.

2 Probability of dam breach

The probability of landslide dam failure is often the first concern for risk management. According to statistics, 50 % of landslide dams will fail within 1 week. The approaches of rigorous stability analysis conventionally used for man-made earth dams are not practical or feasible because the required data for these analyses are often unavailable or insufficient. The results of rigorous stability analysis of an earth dam are sensitive to the input mechanical properties of the dam materials (Evans et al. 2011). However, it is difficult to characterize the required mechanical properties of the dam materials in time. In most cases, the hazard assessment must be conducted quickly; assessment using certain geomorphic approaches may be more practically applicable. Several models of this type are available for classifying the stability of landslide breaches on the basis of geomorphic variables (Costa and Schuster 1988; Ermini and Casagli 2003; Korup 2004; Dong et al. 2009, 2011a, b).

Ermini and Casagli (2003) used the dimensionless blockage index, DBI $= \log\left(\frac{A \times H}{V_d}\right)$ to predict the stability of a landslide dam. This DBI index contains three geomorphic variables, including the blocked catchment area A, the dam volume V_d, and the dam height H. An inventory of 84 landslide dam cases, including both stable and unstable cases, showed that a landslide dam would be stable if DBI < 2.75 and unstable if DBI > 3.08. Tabata et al. (2002) compiled an inventory of 46 Japanese landslide dam cases with comprehensive information of the landslide dams, as shown in Fig. 1. Using the inventory of Tabata et al. (2002) and discriminant analysis, Dong et al. (2009) screened out the main geomorphic parameters that affect the stability of landslide dams and established discriminant models with four major geomorphic parameters. These geomorphic parameters included the peak discharge P flowing into the barrier lake and the common geometric parameters of the landslide dam, such as the length L, the width W, and the height H of the dam. The following equation is their discriminant model, *PHWL*_Dis with *P, L, W*, and *H*.

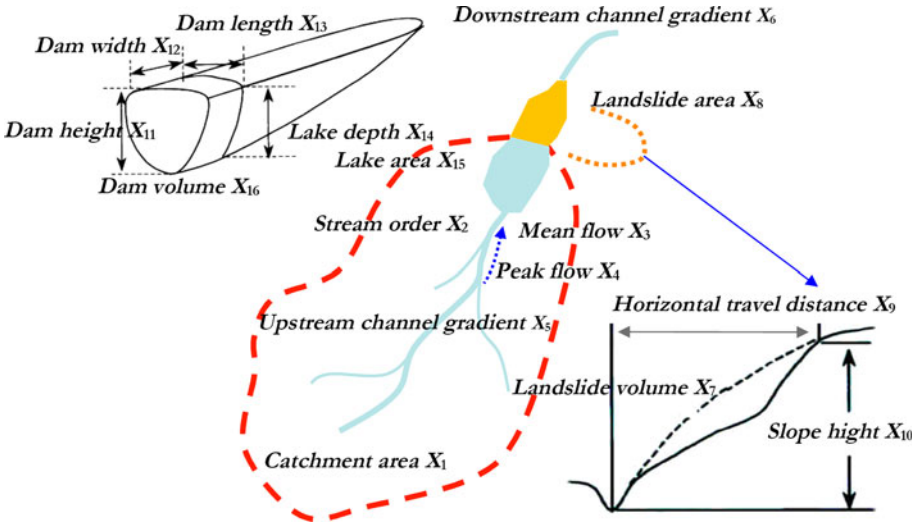

Fig. 1 Illustration of geomorphic parameters included in the inventory of Tabata et al. (2002)

$$D_s = -2.94\log(P) - 4.58\log(H) + 4.17\log(W) + 2.39\log(L) - 2.52 \quad (1)$$

However, the peak discharge is not always available or predictable soon after the formation of a landslide dam. Consequently, the area of the blocked catchment A is often preferable to the peak discharge P for practical application of discriminant models. The following equation is the discriminant model, *AHWL*_D containing *A, L, W,* and *H*.

$$D_s = -2.62\log(A) - 4.67\log(H) + 4.57\log(W) + 2.67\log(L) + 8.26 \quad (2)$$

The unit of the catchment area A in (2) is m^2. For these discriminant models, the discriminant score D_s indicates the stability state of a landslide dam. For a stable landslide dam, the score D_s is positive; for an unstable dam, D_s is negative. The required geomorphic parameters in the discriminant model can be determined from a field survey or estimated using remote sensing images. If a field survey cannot be conducted in time, it is possible to estimate the required geomorphic parameters using procedures based on orthoimages produced from aerial photos or satellite photos with a pre-landslide digital elevation model (DEM) or terrain contours (Dong et al. 2012). Dong et al. (2009) indicated that the discriminant models, *PHWL*_D and *AHWL*_Dis, correctly classified the stability of landslide dams by up to 88.6 and 86 %, respectively, for the cases in the inventory of Tabata et al.

Using the same set of Japanese data, Dong et al. (2011a, b) further developed logistic regression models to predict the stability state of a landslide dam. Logistic regression is a useful statistical approach when the dependent variable is categorical (e.g., stable or unstable); the independent variables can be either categorical or numerical (Menard 2002). The *PHWL_Log* model is expressed as a function of *P*, *L, W,* and *H*.

$$L_s = -2.55\log(P) - 3.64\log(H) + 2.99\log(W) + 2.73\log(L) - 3.87 \quad (3)$$

The *AHWL_Log* model is expressed as a function of *A, L, W*, and *H*.

$$L_s = -2.22\log(A) - 3.76\log(H) + 3.17\log(W) + 2.85\log(L) + 5.93 \quad (4)$$

The dependent variable L_s in these logistic regression models is called "logit". The logit L_s is a measure of the total contribution of all independent variables (*P*, *L*, *W,* and *H*) or (*A*, *H*, *W,* and *L*). A landslide dam with $L_s > 0$ is classified into the stable group and that with $L_s < 0$ is classified into the unstable group. Moreover, the failure probability of a landslide dam can be related to the logit L_s using the following equation (Menard 2002).

$$P_f = e^{-L_s}/(1 + e^{-L_s}). \quad (5)$$

When $L_s = 0$, the probability of a landslide dam failure is 50 %. For a landslide dam with $L_s > 0$, the probability of landslide dam failure P_f is less than 50 %, and vice versa.

This study suggests the use of the logistic regression models for the estimation of the dam-breach probability P_f. Furthermore, the level of P_f is classified into various levels, as follows: extremely low ($P_f \leq 10$ %), low (10 % $\leq P_f \leq$ 40 %), middle

Table 1 Classification of dam-failure probability

Level of dam-failure probability	P_f (%)	Description of flood disaster
Extremely low (I)	0–10	Almost not occur
Low (II)	11–40	Seldom occur
Middle (III)	41–60	May occur about half
High (IV)	61–90	Often occur
Extremely high (V)	Over 90	Always occur

(40 % $\leq P_f \leq$ 60 %), high (60 % $\leq P_f \leq$ 80 %), and extremely high ($P_f \geq$ 80 %). Table 1 shows various levels of dam-failure probability and their corresponding definitions.

3 Assessment of upstream inundation hazard

3.1 Quick assessment

After a landslide dam is formed, the upper reach of the landslide dam is inevitably exposed to inundation threat because of the rise in the water level in the barrier lake dammed by the landslide dam. A quick assessment of the covered area of inundation can be conducted soon after the determination of the correct location of the landslide dam and the elevation of the dam crest. With the pre-landslide DEM or terrain contours, the boundary of the to-be-affected region of inundation can be identified along the contour corresponding to the dam-crest elevation. A geographic information system (GIS) platform can expedite the involved work when it is available and usable. Dong et al. (2012) proposed a method to quickly assess the geometry from remote sensing images. Various types of facilities, infrastructures, resident housing, roadways, and bridges can also be identified from maps and orthoimages with land-use information.

The time of incoming inundation can be predicted if the in-flow discharge is predictable. An alternative approach can be used if the in-flow discharge is not available or cannot be determined in time. With the DEM, the relation between water storage volume and water level can be established. The continuous change in the water volume can be determined if the water level in the barrier lake is continuously monitored or a series of multi-staged satellite images are available. With the difference in the water storage volume ΔV_l and the time increment ΔT, the in-flow discharge Q can be estimated using $Q = \Delta V_l/\Delta T$. Alternatively, it is possible to estimate the maximal in-flow discharge by assuming that the unit catchment area in the upper reaches can bring a constant maximal discharge into the barrier lake and the maximal in-flow discharge is proportional to the catchment area in the upper stream of the landslide dam.

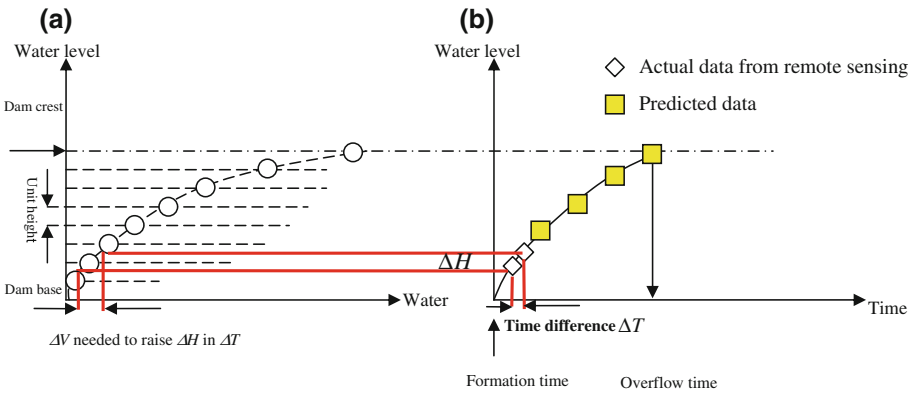

Fig. 2 Schematic illustration of the estimation for in-flow discharge and overtopping time in quick assessment

The time of overtopping from a landslide dam is equivalent to the fill-up time of the barrier lake. With an estimated in-flow discharge, the elapsed time for the fill-up of the barrier lake (i.e., the remaining time for overtopping to occur) can be estimated. Figure 2 shows the schematic illustration of this approach. Figure 3 shows the flow chart of procedures for the quick assessment of the inundation hazard in the upstream of a landslide dam.

3.2 Detailed assessment

If a landslide dam remains stable for a certain period, sufficient time may be available to collect the detailed terrain and hydrological information in its upper reaches. A detailed assessment of the inundation hazard in the upper reaches can be conducted after the detailed information is obtained. The required information may include the correct geometry of the landslide dam, the cross sections of the river channel, the measured water stage that varies with time, and the measured or predicted rainfall intensity.

The relation between the runoff intensity and the in-flow discharge can be determined using rainfall-runoff models. Subsequently, the average runoff intensity that causes overtopping can be assessed for an elapsed time. Furthermore, flooding analysis using appropriate software, such as *SOBEK-2D* (Deltares Systems 2012), can accurately predict the progressive rise of the water stage and the range of inundation in the upstream corresponding to an input intensity of rainfall in the upper reach. The details of the terrain model, including the correct cross sections of the river channel, are required for the analysis. The results of flooding analysis can forecast the covered area of inundation and the distribution of the flooding depth. With detailed maps of land uses and infrastructures, the affected area and the possible effects can be assessed for risk management of the flooding hazard in the upper reaches. The classification of the flooding hazard is presented in Sect. 5.

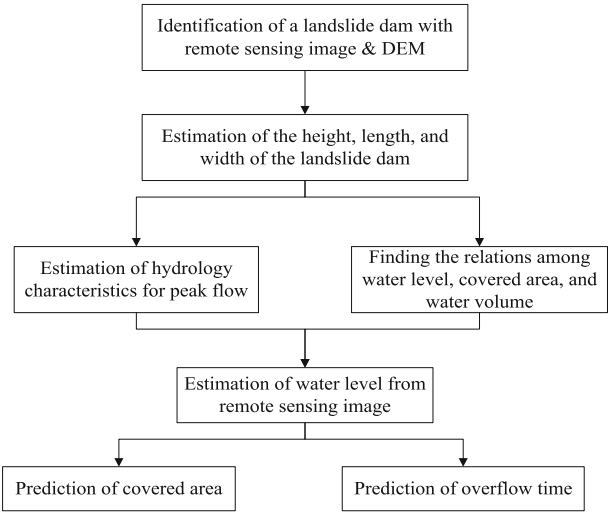

Fig. 3 Flow chart of procedures in the quick assessment for the inundation hazard in the upstream of a landslide dam

4 Assessment of downstream inundation hazard

4.1 Quick assessment

The available time for the response of risk mitigation and management is often limited. For the early phase, a quick assessment must not require a long time to complete and must not require excessive detailed data, which are difficult to collect in a short time. A quick approach is preferable when the data collection is incomplete or the risk assessment must be conducted quickly. For example, a geomorphic approach may be used to roughly estimate the peak outflow discharge following a dam breach using only geomorphic parameters (Walder and O'Connor 1997; Costa 1985; Costa and Schuster 1988; Peng and Zhang 2012).

To minimize the required time for the assessment of the downstream flooding hazard on the basis of hydraulics, a new strategy is proposed to prepare the result of dam-breach analyses in advance. Therefore, we completed a series of dam-breach analyses for various combinations of geomorphic parameters of dams using the BREACH software (Fread 1988). These analyses calculated the hydrograph of outflow discharge during the dam-breach process and enabled the determination of the peak outflow. Based on the results, we constructed a series of charts to estimate the peak flow outburst from a breached dam. Figure 4 shows an example chart that shows the peak outburst flow Q_m obtained from a dam-break analysis for a prescribed set of geomorphic parameters. For this chart, the upstream dam slope S_u was 1/5, the downstream dam slope S_d was 1/5, and the inflow discharge Q was 3,000 m^3/s; the five curves corresponded to the lake-water storage volume V_l, that is, 5, 10, 20, 30, and 40 million m^3, respectively. The abscissa is the dam height, H_d, whereas the ordinate is the peak outflow discharge from the breached dam. In general, a landslide dam with a gentler slope tends to breach slower; consequently, the peak discharge tends to be smaller. A larger V_l results in a larger peak outburst discharge.

A set of charts were prepared through a series of dam-break analyses for landslide dams with various combinations of geomorphic parameters, which contained various ranges of S_u (1/2, 1/3, 1/4, and 1/5), S_d (1/2, 1/3, 1/4, and 1/5), H_d (from 10 m to 70 m, with the interval 10 m), V (5,10,20,30 and 40 million m^3), and Q (500, 1,000, 2,000, 3,000, 4,000, 5,000, 7,500, and 10,000 m^3/s). The applicable charts were produced in advance and are

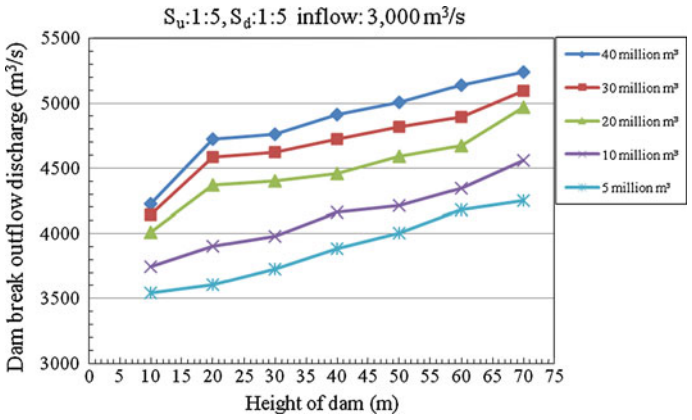

Fig. 4 An example chart for the estimation of peak outburst flow due to landslide dam breach

useful for the estimation of peak outburst discharge when a landslide dam occurs with previously estimated relevant geomorphic parameters. Because an actual landslide dam may not have the same combination of geomorphic parameters as one of the prepared combinations, the estimation of peak outburst discharge can be obtained through a proper interpolation of the results from the charts with the combinations of geomorphic parameters bounding the actual parameters.

For a well-managed river system, the allowable discharge Q_a for every river section must be analyzed and pre-determined for river management. In this study, a flooding hazard index was defined as $I_{db} = Q_m/Q_a$ to assess the level of downstream flooding hazard caused by a dam breach. For a relatively low value of I_{db}, the chance of flooding may be low. For I_{db} close to or larger than 1.0, the potential for flooding is relatively high. For quick assessment of downstream inundation, we propose the use of the I_{db} index for the quick assessment of downstream flooding hazard. As shown in Table 2, five levels of flooding hazards were defined according to the range of I_{db} as follows: extremely low (level I) for $I_{db} = 0.0$–0.10, low (level II) for $I_{db} = 0.11$–0.40, middle (level III) for $I_{db} = 0.41$–0.60, high (level IV) for $I_{db} = 0.61$–0.90, and extremely high (level V) for $I_{db} > 0.90$. The levels of flooding hazards were classified according to Garvey and Lansdowne (1998).

4.2 Detailed assessment

When a landslide remains stable for a sufficient time to collect the required data, it is feasible to perform a detailed dam-breach analysis and flooding analysis for the downstream regions. The implementation of these analyses requires various information as follows: (1) the hydrological characteristics, (2) the relations among water stages, water covered area, and water storage volume in the barrier lake, (3) the material characteristics and properties of the landslide dam, including the strength parameters and grain size distribution, and (4) the river cross sections in the downstream. Figure 5 shows the flow chart illustrating the procedures of the analyses and the required input data.

A proper software, such as *BREACH* (Fread 1988), may be used to perform dam-breach analysis. The *BREACH* software can obtain the outflow discharge hydrograph and progressive widening of the breached section in the process of a dam breach. The required input data for the analysis include the unit weight, the mean grain size, the strength parameters (e.g., c and ϕ) of the dam material, the geometry of the landslide dam, the relations among water stages, covered area and water storage volume, and the inflow discharge from the upper reaches. The dam-breach analysis can obtain the results of the outflow discharge hydrograph (i.e., the time history of discharge outburst from the breached dam) as well as the progressive change in the cross sections of the breached dam.

Table 2 Classification of flooding hazard level through I_{db}

Classification of flood hazard	I_{db}	Description of flood disaster
Extremely low (I)	0–0.10	Almost not occur
Low (II)	0.11–0.40	Seldom occur
Middle (III)	0.41–0.60	May occur about half
High (IV)	0.61–0.90	Often occur
Extremely high (V)	Over 0.90	Always occur

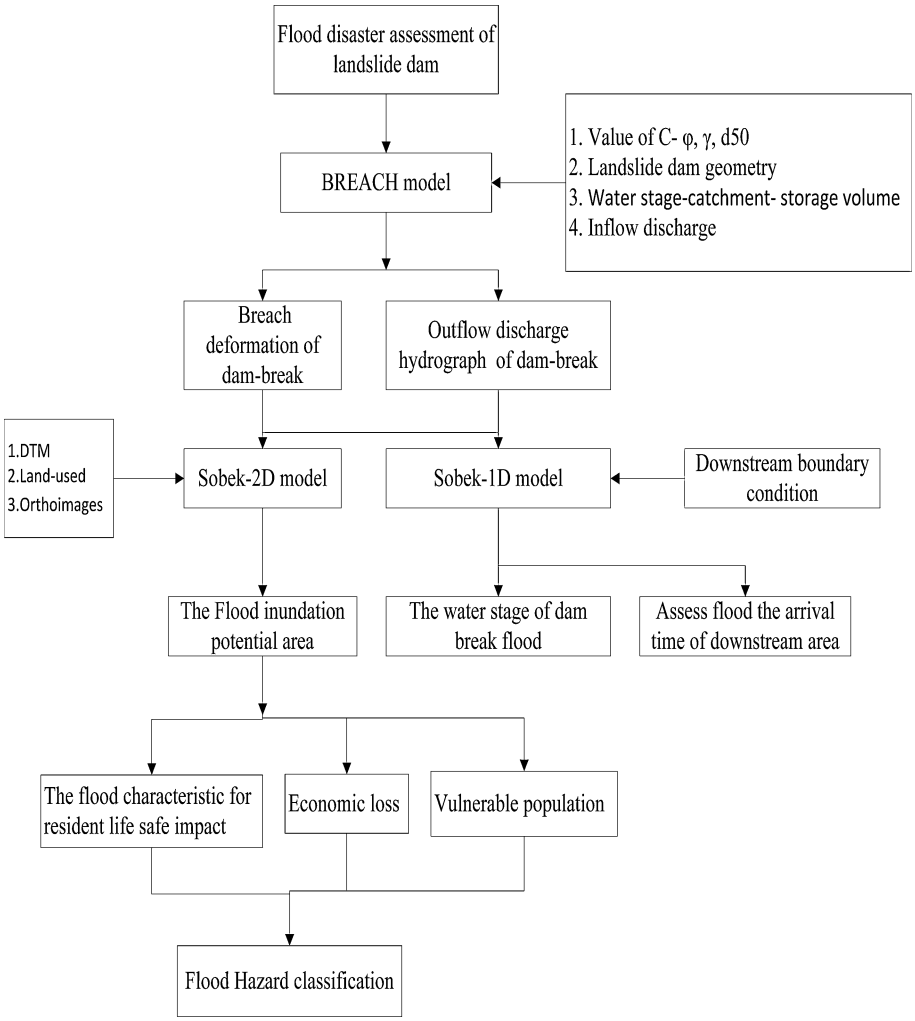

Fig. 5 Flow chart of detailed assessment for downstream inundation

With the calculated outflow discharge hydrograph, one-dimensional flooding analysis using an appropriate software, such as *Sobek-1D* (Deltares Systems 2012), can be used to simulate the variation of water stages caused by the discharge outburst from the breached dam and calculate the arrival time of flooding. This analysis requires the downstream boundary conditions of the water levels. Furthermore, two-dimensional flooding analysis using an appropriate software, such as *Sobek-2D* (Deltares Systems 2012), can be used to calculate the flooding area, the distributions of water depth, and flow velocity. An analysis using *Sobek-2D* requires input data of a detailed digital terrain model. With the calculated results of the flooding area, water depth, flow velocity, and water-rise rate, the flooding hazard can be assessed and classified by considering the vulnerable population and economic loss. The assessment of flooding hazard must identify the land-use type and population distribution in the flooding area. High resolution orthoimages and an appropriate

GIS can help to recognize the affected objects within the flooding zones. The approach of hazard classification is discussed in the following section.

5 Classification of inundation hazard and risk

5.1 Flooding hazard index

To evaluate the level of flooding hazard that threatens human life, this study considered flooding variables including the flooding depth, the runoff velocity, and the water-rise rate. These variables substantially affect the survival of humans when encountering a flood. For classification, a simplified approach is to introduce a flooding hazard index, H_{db}, defined as follows:

$$H_{db} = \alpha \times WD + \beta \times WV + \gamma \times WR \tag{6}$$

Three sub-indexes, *WD*, *WV*, and *WR,* are used to quantitatively classify the level of danger caused by the flooding depth, runoff velocity, and water-rise rate, respectively. All of these sub-indexes are within 0.0 and 1.0. α, β, and γ represent the weighting coefficients for *WD*, *WV*, and *WR*, respectively. The assignments of the sub-indexes and the weighting coefficients can be determined through a procedure using the analytical hierarchy process

Table 3 Sub-index of flooding depth WD

Range of flood depth	Value of WD	Description
Under 0.29 m	0–0.49	Under children's knee
0.3–0.49 m	0.50–0.69	Reach adult's knee, hard to walking and influence the car driving
0.5–0.99 m	0.70–0.89	Reach adult's waist, unable to walk or drive
1.0–2.99 m	0.90–0.99	Reach adult's chest, life threat
Over 3.0 m	1.0	Reach the second floor

Table 4 Sub-index of flow velocity WV

Range of flow velocity	Value of WV	Description
Under 0.49 m/s	0–0.69	Rescue team can carry on rescue operations smoothly as water depth is under waist
0.5–1.49 m/s	0.70–0.99	Rescue team can carry on rescue operations smoothly as water depth is under knee
Over 1.5 m/s	1	Rescue team cannot carry on rescue operations

Table 5 Sub-index of water-rise rate WR

Range of flood rising rate	Value of WR	Description
Under 0.74 m/h	0–0.49	Retreat time over 2 h
0.75–1.49 m/h	0.5–0.69	Retreat time within 1 and 2 h
1.5–3.0 m/h	0.7–0.99	Retreat time within 0.5 and 1 h
Over 3.0 m/h	1	Retreat time <0.5 h

Table 6 Classification of flooding hazard level through H_{db}

Classification of flood hazard	H_{db}	Description of flood disaster
Extremely low (I)	0–0.10	Almost not occur
Low (II)	0.11–0.40	Seldom occur
Middle (III)	0.41–0.60	May occur about half
High (IV)	0.61–0.90	Often occur
Extremely high (V)	Over 0.90	Always occur

(AHP). The description of AHP is beyond the scope of this paper and can be referred to in Saaty (2004). An example of AHP for the classification of common flooding hazards is used by the Water Resources Agency (WRA) in Southern Taiwan (Water Resources Agency 2011). They suggested the values of the sub-indexes, *WD*, *WV*, and *WR,* for various conditions of flooding depth (Table 3), runoff velocity (Table 4), and water-rise rate (Table 5). They also suggested using the following values of weighting coefficients: $\alpha = 0.24$, $\beta = 0.44$, and $\gamma = 0.32$. This study adopted these suggested values of the sub-indexes and weighting coefficient. The values of *WD*, *WV*, and *WR* corresponding to the calculated results of flooding depth, runoff velocity, and water-rise rate can be determined from the results of breach analysis and flooding analysis; consequently, the flooding hazard index H_{db} can be evaluated. For the detailed assessment of downstream inundation, we classified the levels of flooding hazards on the basis of H_{db}. As shown in Table 6, the levels of flooding hazards were defined according to the range of H_{db}. The flooding hazards were classified into five distinct levels as follows: extremely low (level I) for $H_{db} = 0.0$–0.10, low (level II) for $H_{db} = 0.11$–0.40, middle (level III) for $H_{db} = 0.41$–0.60, high (level IV) for $H_{db} = 0.61$–0.90, and extremely high (level V) for $H_{db} > 0.90$.

5.2 Vulnerable population and economic loss

For simplicity, the vulnerable population was defined as the number of senior citizens over the age of 65 or those with disabilities. We assumed that each household in any location with a flooding depth of over 0.5 m had two vulnerable people.

Various land-uses may have differing tolerances to the flooding depth; therefore, the assessment of economic loss caused by flooding must be based on the type of land use. Assessment of economic loss can be performed by assigning a nominal loss for each type of land use and various depth ranges of inundation.

Table 7 Classification of the flooding risk associated with a landslide dam

Classification of flooding risk	Level of dam-failure probability				
	V	IV	III	II	I
Level of flooding hazard (H_{db} or I_{db})					
V	Extremely high	Extremely high	High	High-middle	Middle
IV	Extremely high	High	Middle-high	Middle	Middle-low
III	High	Middle–high	Middle	Middle-low	Low
II	High-middle	Middle	Middle-low	Low	Extremely low
I	Middle	Middle-low	Low	Extremely low	Extremely low

5.3 Classification of downstream flooding risk

The potential risk of the flooding hazard caused by a breach of a landslide dam depends on the failure probability of the dam and the resulting flooding hazard. Therefore, the risk of flooding associated with the occurrence of a landslide dam can be classified according to the combined conditions of the level of dam-breach probability and the level of flooding hazard.

The level of the flooding hazard can be classified either by I_{db} obtained from a quick assessment (Table 2) or by H_{db} obtained from a detailed assessment (Table 6). A simplified and feasible approach for the classification of the risk level is to use the concept of risk matrix (Garvey and Lansdowne 1998). Table 7 shows the proposed matrix of classification for downstream flooding risk from a landslide dam. The horizontal (row) is the level of the dam-failure probability, whereas the vertical (column) is the level of the flooding hazard. There are five levels of dam-failure probability and five levels of flooding hazard. Depending on their combination, the downstream flooding risk is classified into seven levels as follows: extremely high (level VII), high (level VI), middle-high (level V), middle (level IV), middle-low (level III), low (level II), and extremely low (level I).

6 Demonstration using a case study

6.1 The Xiaolin landslide dam

Typhoon Morakot hit southern Taiwan on August 8, 2009, and caused more than 2,100 mm of rainfall in 4 days; the peak hourly rainfall intensity was nearly 100 mm/h. The heavy rainfall triggered 17 large landslides and resulted in the formation of several landslide dams, including the Xiaolin landslide dam located near the Xiaolin Village in southern Taiwan. Near Xiaolin, heavy rainfall resulted in a large landslide along a creek and subsequently blocked the Cishan River to form the Xiaolin landslide dam (Dong et al. 2011a, b; Li et al. 2011); this landslide was catastrophic and caused more than 400 casualties. By analyzing the broad-band seismic signals, Feng (2011, 2012) indicated that the time of the landslide dam formation and dam breach was 6:16 AM and 7:40 AM, respectively. Therefore, the landslide dam breached 84 min after its formation. Figure 6 shows the post-landslide orthoimage (Aerial Survey Office, Forestry Bureau of Taiwan, ASOFB). Dong et al. (2011a, b) conducted post-event reconstruction of the geometry of the landslide dam. Based on their reconstruction, the major geomorphic parameters of the landslide dam were estimated as follows: catchment area $A = 354$ km^2, dam length $L = 370$ m, dam width $W = 1{,}550$ m, dam height $H_d = 44$ m, upstream dam slope $S_u > 1/5$, and downstream dam slope $S_d > 1/5$. They also indicated that overtopping dominated the failure process of this heavy-rainfall-induced landslide dam. Although the landslide dam breached shortly after its formation, this case was used for the demonstration of the proposed method.

6.2 Assessment of upstream inundation

6.2.1 Quick assessment

Based on the reconstruction of landslide dam geometry by Dong et al. (2011a, b), the saddle point of the dam crest (which is the estimated lowest elevation of dam crest) was

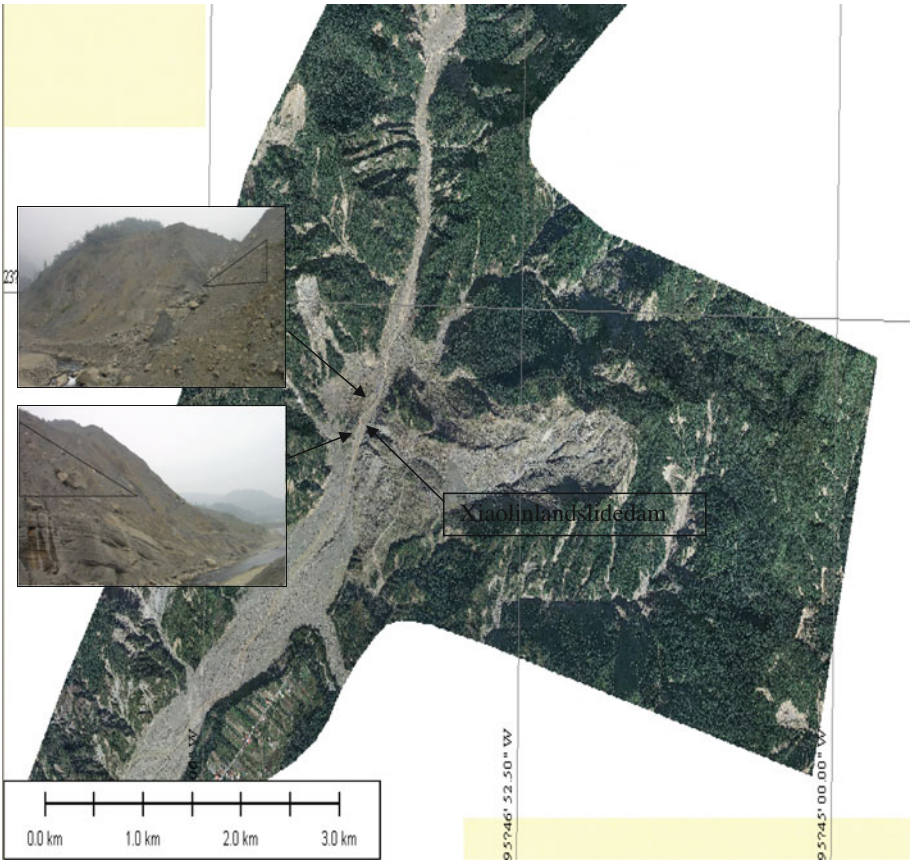

Fig. 6 Post-landslide orthoimage near the Xiaolin landside dam

approximately 415 m and can be considered the elevation of the water stage when overtopping started. For quick assessment, the region enclosed by the contours corresponding to 415 or 420 m in the upstream of the landslide dam can be assumed as the potential area of inundation. Figure 7 shows the regions surrounded by the contours of 415 and 420 m. Figure 8 is the orthoimage overlapped with these contours. With the land-use information and detailed map, the affected infrastructures and objects potentially exposed to the threat of inundation can be identified in advance.

Based on empirical hydrology in southern Taiwan, we assumed that each km^2 of the catchment area in the upper reaches can bring a maximal discharge of 10 m^3/s into the barrier lake; thus, the estimated in-flow discharge was 3,540 m^3/s because the area of the upstream catchment was 354 km^2. Figure 9 shows the relations among the water depth, water covered area, and water storage volume of the barrier lake. The estimated storage capacity of the barrier lake corresponding to the elevation of the dam crest was 1.8×10^7 m^3. Based on the storage capacity and the in-flow discharge, the elapsed time for overtopping was approximately 80 min. The landslide dam breached 84 min after its formation (Feng 2011, 2012). If the landslide dam did not breach that quickly, the information from a quick assessment would be useful for action-planning and decision-making in a short time after the occurrence of a landslide dam to prevent disaster.

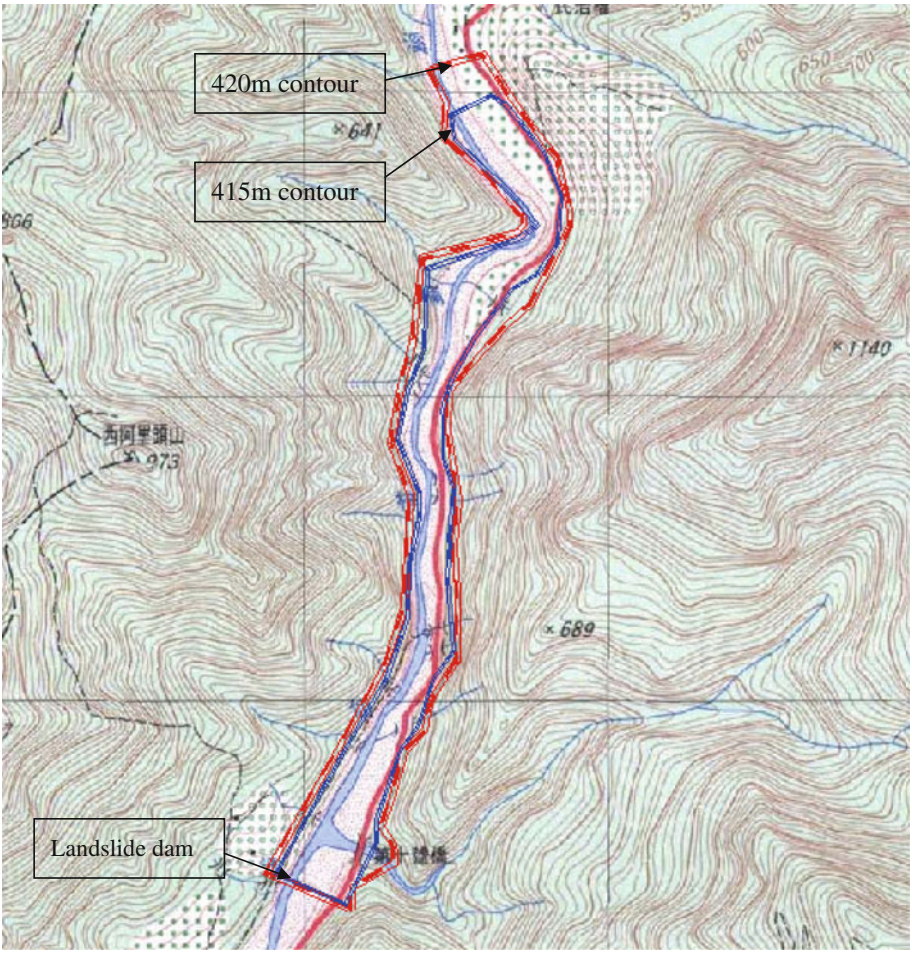

Fig. 7 Pre-landslide contours in the region of the landslide dam

6.2.2 Detailed assessment

With the DEM of the upper reaches and the recorded hydrological data in the Morakot typhoon as the rainfall-runoff model, we conducted two-dimensional flooding analysis and obtained the results of the inundation area with the calculated flooding depth, run-off velocity, and water-rise rate. Figure 10 shows the flooding area and depth in the upstream of the landslide dam at various elapsed times obtained from the flooding analysis using *Sobek-2D*. Ten minutes after dam formation, the water level increased to 389 m. Thirty minutes after dam formation, the water level increased to 400 m. Fifty minutes after dam formation, the water level reached 415 m and exceeded the elevation of the dam crest. Thus, overtopping would occur 50 min after the formation of a dam if the rainfall conditions are the same as those of the Morakot typhoon. The maximal calculated flooding depth, runoff velocity, and water-rise rate on the main roadways within the flooded regions were 22.9 m, 10.4 m/s, and 22.9 m/h, respectively; the WD, WV, and WR sub-indexes must be 1.0 by using Tables 3, 4, and 5. Consequently, the flooding hazard index H_{db} was

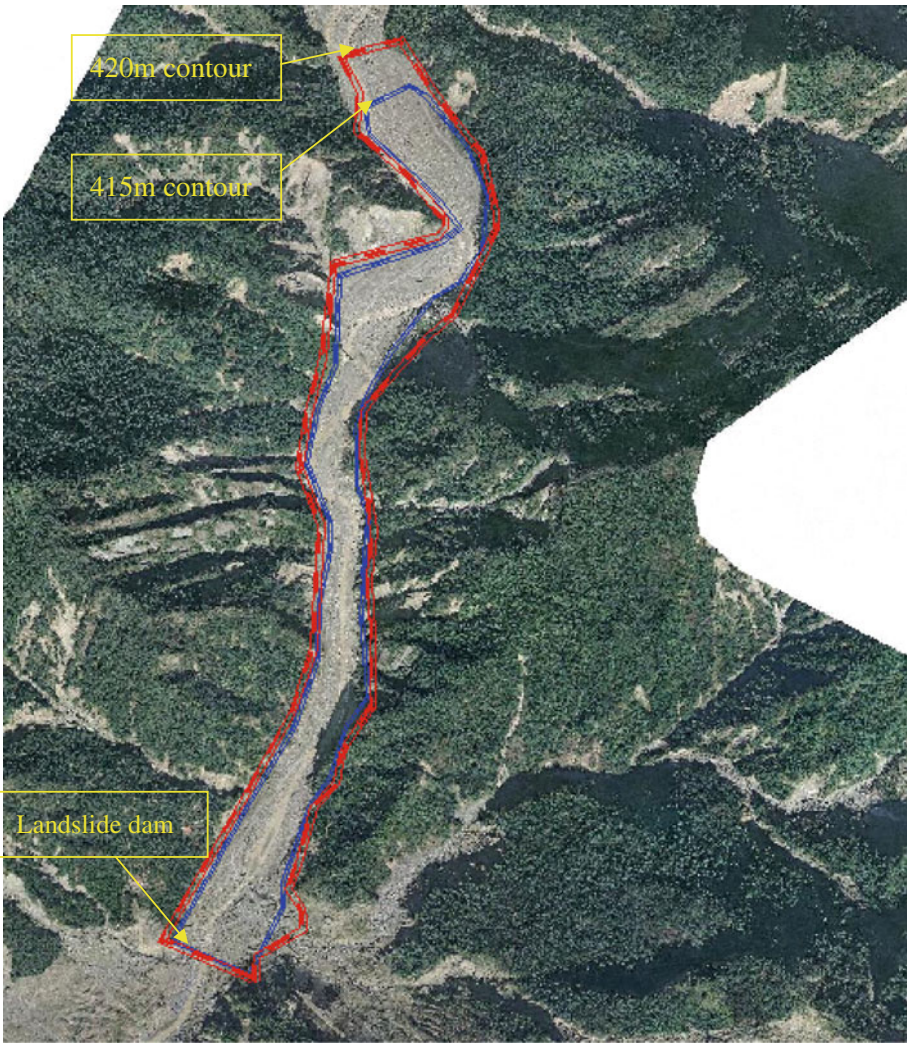

Fig. 8 The orthoimage with the overlapped contours of 415 and 420 m

1.0. Hence, the level of flooding hazard for the upstream of the landslide dam was extremely high (level V).

6.3 Assessment of downstream inundation

6.3.1 The breach probability of the dam

Using relevant geomorphic parameters and (4), the calculated L_s was −1.79; the corresponding dam-failure probability P_f, calculated using (5), was 86 %. Therefore, the level of dam-failure probability was extremely high (level V).

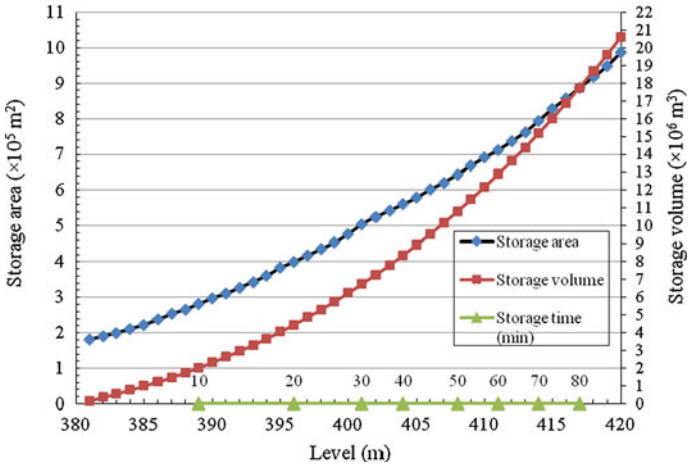

Fig. 9 Relations among water stage, covered area and storage volume of the barrier lake

6.3.2 *Assessment of flooding hazard and risk*

6.3.2.1 Quick assessment Both the downstream and upstream slopes of the landslide dam were steeper than 1/5, but flatter than 1/2. Figure 4 can be used to estimate the peak outburst discharge after the breach of the landslide dam. As described in Sect. 6.2, the estimated in-flow discharge was 3,540 m^3/s and the storage capacity of the barrier lake was 1.8×10^7 m^3. Using Fig. 4, the peak outburst discharge corresponding to these hydrological variables can be obtained through interpolation; the peak discharge was approximately 4.400 m^3/s. For example, the allowable discharge was 3,770 m^3/s in the river section near the Xiaolin Village. Thus, the flooding hazard index was $I_{db} = 4{,}400/3{,}770 = 1.17 > 1.0$. Therefore, the level of flooding hazard was extremely high (level V) for this river section. Combining the level of dam-failure probability and the level of flooding hazard, the level of the flooding risk in this river section was extremely high.

6.3.2.2 Detailed assessment For detailed assessment, the breach analysis was first conducted using the following input parameters: (1) the unit weight, the mean grain size, and the strength parameters, and the geometry of the landslide dam; (2) the relation among water stages, covered area, and storage volume; and (3) the inflow discharge. A breach analysis was conducted using the recorded data for the Morakot typhoon as the rainfall-runoff model. Figure 11 shows the calculated hydrographs of inflow and outflow discharges obtained by the dam-breach analysis. As shown in this figure, the peak in-flow discharge was approximately 3,100 m^3/s, whereas the peak outflow discharge was approximately 4,350 m^3/s.

The calculated results of the transient discharge from the breach analysis were used as the upstream boundary condition in the subsequent flooding analysis for the analyses using *Sobek-1D* and *Sobek-2D*. The water stage measured at the hydro-station near the Liling bridge (52.1 km downstream of the Xiaolin) was used as the downstream boundary condition in the analyses. Figure 12 shows the hygrograph of the recorded water level at the hydro-station. The one-dimensional flooding analysis using *Sobek-1D* provided the results of the flood arrival time to the downstream villages (as shown in Table 8). For example,

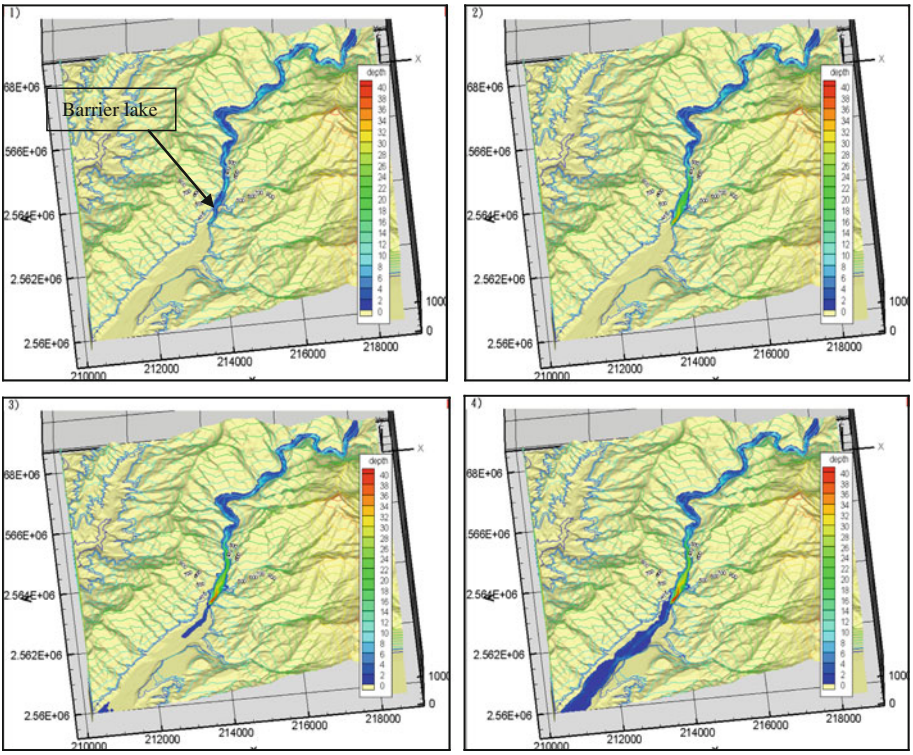

Fig. 10 Time variations of the inundation area and depth in the upstream of the Xiaolin landslide dam: (*1*) immediate after dam formation; (*2*) 30 min after dam formation; (*3*) 50 min after dam formation; and (*4*) 1 h after dam formation

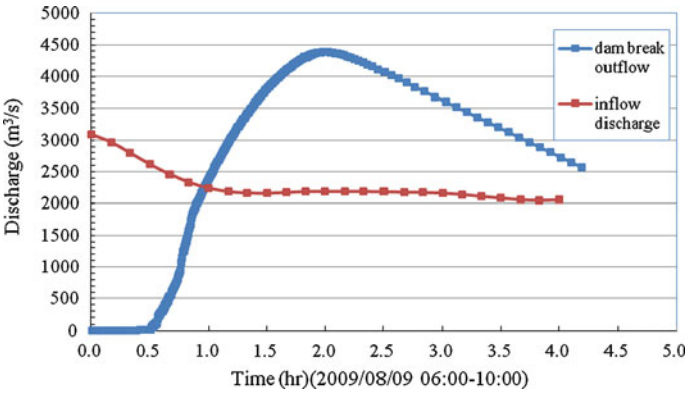

Fig. 11 Flow discharge hydrograph obtained from dam-break analysis for Xiaolin landslide dam

the flood will arrive at the Dongchang (located approximately 47.5 km downstream of the landslide dam) in 2 h. As shown in Fig. 13, the analysis using *Sobek-2D* obtained the area of inundation. The flooding analysis enables the calculation of flooding depth, run-off

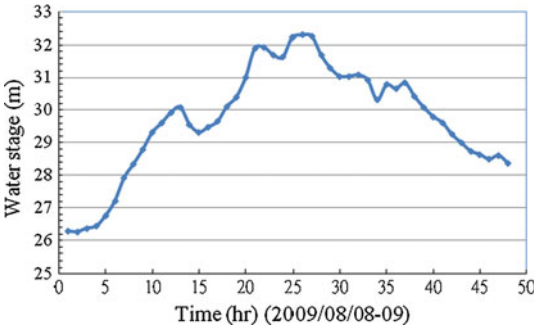

Fig. 12 Downstream boundary condition for the SOBEK models

velocity, and water-rise rate for the assessment of flooding hazard. Table 9 shows the flooding depth, run-off velocity, and water-rise rate and their corresponding sub-indexes (*WD*, *WV*, and *WR*) at ten downstream villages of the Xiaolin landslide dam. The flooding hazard index H_{db} for each village was evaluated using (6). For example, the calculated results for Xiaolin (i.e., the closest village to the landslide dam) were as follows: the flooding depth was nearly 23 m, the runoff velocity exceeded 10 m/s, and the water-rise rate was above 20 m at the main roadway connecting this village; thus, the sub-indexes (*WD*, *WV*, and *WR*) must be 1.0 by using Tables 3, 4, and 5. Table 9 shows that, once the landslide dam breaches, the level of flooding hazard for the Xiaolin village next to the landslide dam would be extremely high (level V); the level of flooding hazard for the three villages (Baolong, Jilai, and Yuemei) in the middle stream would be extremely low (level I); and the level of flooding hazard for the three villages (Yonghe, Dongchang, and Zhonghe) in the downstream would be low(II), extremely high (level V), and high (level IV), respectively.

6.3.3 Classification of flooding risk

Regarding the execution of evacuation and rescue operations, this study suggests the use of the inferior situations of flooding depth, run-off velocity, and water rising rate at the main roadway in each village to assign the sub-indexes, *WD*, *WV*, and *WR*. The flooding hazard indexes H_{db} for the seven villages listed in Table 9 range from 0 to 1.0.

Table 8 Flood arrival time obtained from 1-D flooding analysis

District	Village	Distance from landslide dam (km)	Flood arrival time (h)
Jiasian	Xiaolin	0	0
	Hean	9.6	0.34
	Baolong	15.7	0.5
Shanlin	Jilai	21	0.67
	Xinzhaung	25.4	0.84
	Yuemei	31.5	1
Qishan	Yonghe	36.6	1.5
	XinShan	42.6	1.67
	Dongchang	47.5	2
Ligang	Zhonghe	52.1	3.17

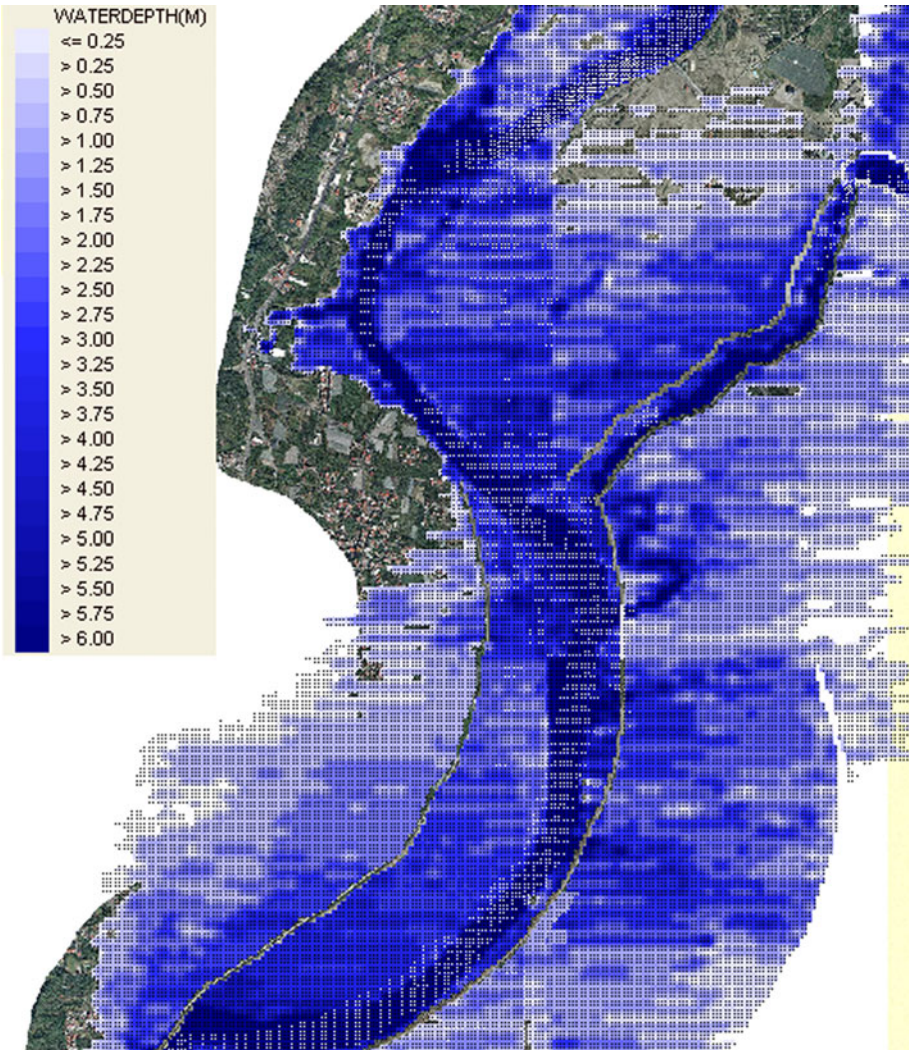

Fig. 13 Inundation distribution in the downstream of Xiaolin landslide dam (from SOBEK-2D flooding analysis)

With the population distribution information, the area must be evacuated and the distribution of vulnerable people that may be trapped in the flooding zone can be identified for disaster mitigation planning. With the land-use information, the potential economic loss can also be assessed according to the flooding condition and the land-use type for each object (e.g., home, commercial building, farm land, industry factory, roadways and bridges) within the region of inundation.

Among the seven villages, two villages were exposed to extremely high levels of flooding hazard (level V), one village was exposed to a high level of flooding hazard (level IV), one village was exposed to a low level of flooding hazard (level II), and three villages were exposed to extremely low levels of flooding hazard (level I). The level of dam-failure

Table 9 Assessment of flooding risk in the downstream of the Xiaolin landslide dam (from detailed assessment)

Village	Xiaolin	Baolong	Jilai	Yuemei	Yonghe	Dongchang	Zhonghe
The failure probability of landslide dam	Extremely high (level V)						
Assessment of flood characteristics at the key roadways							
Maximum flood depth (m)	22.91	0	0	0	0.29	9.65	7.58
WD value	1	0	0	0	0.47	1	1
Maximum flow velocity (m/s)	10.37	0	0	0	0.2	1.08	1.71
WV value	1	0	0	0	0.28	0.75	1
Maximum flood rising rate (m/h)	22.91	0	0	0	0.29	9.44	4.58
WR value	1	0	0	0	0.19	1	1
Flooding hazard (H_{db})	1 (V)	0 (I)	0 (I)	0 (I)	0.29 (II)	0.89 (V)	1 (IV)
Level of flooding risk	Extremely high	Middle	Middle	Middle	High-middle	Extremely high	Extremely high

probability was extremely high (level V). By combining the level of p_f and the level of H_{db} (Table 7), the levels of flooding risk in each village can be evaluated (as shown in the last column of Table 9). The level of flooding risk for the Xiaolin village was extremely high. For the three villages in the middle stream, the level was middle. For the three villages in the downstream, the level in Yonghe was high-middle, whereas the other two villages had extremely high levels of flooding risk.

6.3.4 Comparison of the results of assessments and reality

To verify the proposed approaches, we compared the results from our assessments and what actually happened in Typhoon Morakot. The assessed level of the failure probability for the Xiaolin landslide dam was extremely high; this was consistent with actual outcome of the dam. The peak outflow discharge into the downstream of Xiaolin on August 9, 2009, was inferred from the water stage measured at the Shanlin Bridge, which is located approximately 30 km downstream of the Xiaolin; this discharge was 3,870 m^3/s at approximately 10AM. To compare the predicted results and what actually happened, the peak outflow discharge obtained from the quick assessment was 4,400 m^3/s, whereas the one obtained from the detailed assessment was 4,350 m^3/s. The levels of flooding risk for the villages listed in Table 9 were further compared with the realistic occurrence of flooding in Typhoon Morakot. Flooding did take place in all of the villages classified as the levels higher than "middle"; whereas no villages with the level "middle" was subjected to inundation.

7 Conclusions

This paper proposes a systematic approach to landslide dam assessment using both quick evaluation and detailed evaluation (if possible). This approach includes the evaluation of

dam-breach probability, the assessment of upstream inundation hazard, the assessment of downstream inundation hazard, and the classification of flooding risk.

After the formation of a landslide dam, the upstream of the dam is exposed to a risk of flooding because of the increase in the water level in the barrier lake. A quick assessment of the range of inundation can be performed after determining the correct location of the landslide dam and the dam-crest elevation; the proposed approach can predict the potential flooding region and estimate the overtopping time. A detailed assessment of the flooding hazard in the upper reaches can be conducted if time is available and sufficient information is collected. Flooding analysis using appropriate software can accurately predict the change in the water stage and the range of inundation to allow assessment of the level of flooding hazard.

The risk of downstream flooding must be evaluated using a joint consideration of the dam-breach probability and the level of flooding hazard. This study used a logistic regression model to evaluate dam-breach probability using only geomorphic parameters. The dam-breach probability calculated from the logistic regression model can be classified into various levels.

The downstream inundation hazard was evaluated by considering the outburst flood from the breached dam. A quick assessment or a detailed assessment can be performed to evaluate flooding hazards. The quick assessment approach uses a potential flooding hazard index, $I_{db} = Q_m/Q_a$, which compares the peak outburst flow Q_m (estimated from a series of available charts) to the allowable discharge Q_a for each river section. Detailed assessment approaches, including dam-breach analysis and flooding analysis, can be conducted if time is available and sufficient data are collected. With the calculated results of flooding analysis, the flooding hazard can be assessed using a flooding hazard index H_{db} by considering relevant factors (including water depth, flow velocity, and water-rise rate). The flooding hazard is classified into various levels regarding the seriousness of flooding with the range of either I_{db} or H_{db}.

The overall risk of a landslide dam on the downstream inundation may be classified according to the level combination of dam-breach probability and flooding hazard. For various combinations, the degrees of flooding risk can be classified into various levels. The example of the Xiaolin landslide dam case study in southern Taiwan demonstrates the applicability of the systematic approach.

Acknowledgments The presented work was supported by the National Science Council, Taiwan (through the grant 99-2625-M-009-004-MY3) and by the Water Resources Agency Ministry of Economic Affairs of Taiwan. These supports are gratefully acknowledged.

References

Costa JE (1985) Floods from dam failures. US Geological Survey, Open-File Report 85–560, 54 pp

Costa JE, Schuster RL (1988) The formation and failure of natural dams. Geol Soc Am Bull 100(7):1054–1068

Cui P, Zhu Y, Han Y, Chen X, Zhuang J (2009) The 12 May Wenchuan earthquake-induced landslide lakes: distribution and preliminary risk evaluation. Landslides 6:209–223

Deltares Systems (2012) http://www.deltaressystems.com/hydro

Dong JJ, Tung YH, Chen CC, Liao JJ, Pan YW (2009) Discriminant analysis of the geomorphic characteristics and stability of landslide dams. Geomorphology 100:162–172

Dong JJ, Tung YH, Chen CC, Liao JJ, Pan YW (2011a) Logistic regression model for predicting the failure probability of a landslide dam. Eng Geol 117:52–61

Dong JJ, Li YS, Kuo CY, Sung RT, Li MH, Lee CT, Chen CC (2011b) The formation and breach of a short-lived landslide dam at Siaolin village. Taiwan—part I: post-event reconstruction of dam geometry. Eng Geol 123(1–2):40–59

Dong JJ, Li YS, Chang CP, Yang SH, Yeh KC, Liao JJ, Pan YW (2012) Deriving landslide-dam geometry from remote sensing images for rapid assessment of critical parameters related to dam-breach hazards. Submitted to Landslides

Ermini L, Casagli N (2003) Prediction of the behavior of dams using a geomorphological dimensionless index. Earth Surf Proc Land 28:31–47

Evans SG, Delaney KB, Hermanns RL, Strom A, Scarascia-Mugnozza G (2011) The formation and behavior of natural and artificial rockslide dams; Implications for engineering performance and hazard management. In Evans SG et al (eds) Natural and artificial rockslide dams. Lecture Notes in Earth Sciences 133, 1, Springer, Berlin Heidelberg

Feng ZY (2011) The seismic signatures of the 2009 Shiaolin landslide in Taiwan. Nat Hazards Earth Syst Sci 11:1559–1569

Feng ZY (2012) The seismic signatures of the surge wave from the 2009 Xiaolin landslide-dam breach in Taiwan. Hydrol Process 26(9):1342–1351

Fread DL (1988) BREACH: An erosion model for earthen dam failures. National Weather Service, Office of Hydrology, Silver Spring

Garvey PR, Lansdowne ZF (1998) Risk matrix: an approach for identifying, assessing, and ranking program risks. Air Force J Logist 22(1):18–21

Korup O (2004) Geomorphometric characteristics of New Zealand landslide dams. Eng Geol 73:13–35

Li MH, Sung RT, Dong JJ, Lee CT, Chen CC (2011) The formation and breaching of a short-lived landslide dam at Hsiaolin village, Taiwan—Part II: simulation of debris flow with landslide dam breach. Eng Geol 123(1–2):60–71

Menard S (2002) Applied logistic regression analysis, 2nd edn. Sage, Thousand Oaks

Peng SM, Zhang LM (2012) Breaching parameters of landslide dams. Landslides 9(1):13–31

Saaty TL (2004) Decision making—the analytic hierarchy and network processes (AHP/ANP). J Syst Sci Syst Eng 13(1):1–35

Schuster RL (1995) Landslide dams—a worldwide phenomenon. J Jpn Landslide Soc 31:38–49

Schuster RL, Costa JE (1986) A perspective on landslide dams. In: RL Schuster (ed) Landslide dams: processes, risk, and mitigation. Am Soc Civ Eng Geotech Spec Publ, vol 3, pp 1–20

Tabata S, Mizuyama T, Inoue K (2002) Natural Landslide Dams Hazards. Kokonshoin, Tokyo (in Japanese)

Walder JS, O'Connor JE (1997) Methods for predicting peak discharge of floods caused by failure of natural and constructed earthen dams. Water Resour Res 33(10):2337–2348

Water Resources Agency, Ministry of Economic Affairs (2011) A demonstration project for producing maps of vulnerability and risk in the Gaoping river, Donggang river, Kaohsiung city and county, and Pingtung county (in Chinese)

Xu Q, Fan XM, Huang RQ, Van Westen C (2009) Landslide dams triggered by the Wenchuan Earthquake, Sichuan Province, south west China. Bull Eng Geol Environ 68:373–386

Yin Y, Wang F, Sun P (2009) Landslide hazards triggered by the 2008 Wenchuan earthquake, Sichuan, China. Landslides 6:139–152